SIGNAL PROPERTIES OF SQUINT MODE BISTATIC SAR

Junjie Wu, Yulin Huang, Jintao Xiong and Jianyu Yang

School of Electronic Engineering
University of Electronic Science and Technology of China
Chengdu, 610054, Sichuan, P.R.China

ABSTRACT

In this paper, the signal properties for the translational invariant case of bistatic Synthetic Aperture Radar (SAR) based on the squint mode are deduced. Bistatic range history, point target response in time and frequency domains, Doppler properties and resolutions are presented in terms of the platform coordinates and the squint angles. The results are valid for large aperture and large squint angles. The accuracy of quadratic approximation in bistatic SAR is also discussed.

***Index Terms*—** Bistatic SAR, squint mode

1. INTRODUCTION

Bistatic Synthetic Aperture Radar (SAR), which uses the separated transmitter and receiver, is receiving considerable attention recently[1][2]. According to the relationship between the transmitter and receiver, the bistatic SAR could be sorted into two types: translational invariant one and translational variant one [3]. Translational invariant means the azimuth velocity vectors of the transmitter and receiver are constant and identical. Furthermore, squint is hardly to be avoided in bistatic case, except both platforms operate in strip modes with the antennas pointing 90° broadside(side-looking). Therefore, the signal properties of bistatic SAR could be analyzed using the methods for squint monostatic SAR.

This paper presents the signal properties including bistatic range history, point target response, Doppler properties and resolutions based on the squint geometry configuration for bistatic translational invariant case, without small angle approximation. The results are general and therefore could provide a thorough understanding of bistatic SAR signal. In addition, the analysis from the squint perspective could provide a new way of thinking to research the bistatic SAR.

The paper is organized as follows: In Section 2, the bistatic translational invariant geometry, the notation and the range history are summarized. The point target response of the bistatic SAR data acquisition system is derived in Section 3 both in time and angle frequency/wavenumber domains. In Section 4, the Doppler properties in bistatic SAR is investigated. Section 5 shows the relations between resolutions and squint angles. Finally, Section 6 gives the conclusions.

2. GEOMETRY CONFIGURATION

2.1. GEOMETRY CONFIGURATION

The bistatic SAR geometry configuration used in this paper is shown in Fig.1, where the indexes "1" and "2"denote transmitter and receiver values, respectively. $\boldsymbol{R}$ is the slant range vector, $\boldsymbol{x}$ is the azimuth vector, x_0 is the aperture center, $\boldsymbol{\xi}(x, y, z)$ is the location vector, θ_s represents the squint angle, and $\boldsymbol{\eta}$ is the baseline vector.

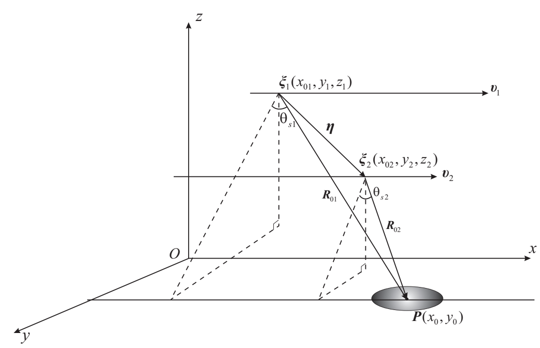

Fig. 1: Bistatic Geometry configuration

Translational invariant means $\boldsymbol{v}_1 = \boldsymbol{v}_2 = \boldsymbol{v}$ =constant and $\boldsymbol{\eta}$ =constant.

2.2. RANGE HISTORY

Apparently, from the bistatic geometry configuration, we can have the range histories of the transmitter and receiver:

$$R_1(x; x_0, y_0) = \sqrt{R_{01}^2 + (x - x_{01} - \Delta x)^2 - 2R_{01}(x - x_{01} - \Delta x)\sin\theta_{s1}} \tag{1}$$

$$R_2(x; x_0, y_0) = \sqrt{R_{02}^2 + (x - x_{02})^2 - 2R_{02}(x - x_{02})\sin\theta_{s2}} \tag{2}$$

where $\Delta x = x_{02} - x_{01}$. Hence, the range history of the bistatic SAR is:

$$R_b(x; x_0, y_0) = R_1(x; x_0, y_0) + R_2(x; x_0, y_0) \tag{3}$$

3. POINT TARGET RESPONSE

The transmitted signal is:

$$s_t(t) = s_0(t) \cdot \exp(j\omega_0 t) \tag{4}$$

where ω_0 is the carrier angular frequency, $s_0(t)$ is the complex envelope of $s_t(t)$. Assuming that the receiver and the transmitter are completely synchronized, the received signal from a point target $\boldsymbol{P}(x_0, y_0)$ with a uniform RCS, after mixed down to the baseband is:

$$\begin{aligned} & s_r(x, t; x_0, y_0) \\ & = s_0[t - t_d(x; x_0, y_0)] \cdot \exp[-j\omega_0 t_d(x; x_0, y_0)] \end{aligned} \tag{5}$$

where $t_d(x; x_0, y_0)$is the bistatic time delay.

Then, using the Principle of Stationary Phase (POSP), the received signal is Fourier transformed on range time domain:

$$S_r(x, \omega; x_0, y_0) = A \cdot \exp[j\psi_{rf}(x, \omega; x_0, y_0)] \cdot S_0(\omega) \tag{6}$$

where $S_0(\omega)$ is the frequency spectrum of $s_0(t)$, and

$$\begin{aligned} & \psi_{rf}(x, \omega; x_0, y_0) \\ & = -\frac{(\omega + \omega_0)}{c} R_1(x; x_0, y_0) - \frac{(\omega + \omega_0)}{c} R_2(x; x_0, y_0) \\ & = \phi_1(x, \omega; x_0, y_0) + \phi_2(x, \omega; x_0, y_0) \end{aligned} \tag{7}$$

Next, using the POSP on azimuth direction, we can get the baseband uncompressed SAR signal in (k_x, ω) domain:

$$S_{2df}(k_x, \omega; x_0, y_0) = A_1 \cdot \exp\{j\psi_b(k_x, \omega; x_0, y_0)\} \cdot S_0(\omega) \tag{8}$$

One of the solutions for (8) can be found in [4]:

$$\psi_b(k_x, \omega; x_0, y_0) = \psi_1(k_x, \omega; x_0, y_0) + \psi_2(k_x, \omega; x_0, y_0) \tag{9}$$

$$\begin{aligned} \psi_1(k_x, \omega; x_0, y_0) = & \phi_1(\hat{x}_1, \omega; x_0, y_0) + \phi_2(\hat{x}_2, \omega; x_0, y_0) \\ & - \frac{1}{2} k_x \hat{x}_1 - \frac{1}{2} k_x \hat{x}_2 \end{aligned} \tag{10}$$

where $\hat{x}_1$ and $\hat{x}_2$ are the points of stationary phase.

The results are:
1) Quasi monostatic term: $\psi_1(k_x, \omega; x_0, y_0)$

$$\begin{aligned} & \psi_1(k_x, \omega; x_0, y_0) \\ & = -\frac{1}{2} \sqrt{\left(\frac{\omega + \omega_0}{c/2}\right)^2 - k_x^2} \cdot (R_{01} \cos\theta_{s1} + R_{02} \cos\theta_{s2}) \\ & - \frac{k_x}{2}(R_{01} \sin\theta_{s1} + R_{02} \sin\theta_{s2}) - \frac{k_x}{2}(x_{01} + x_{02}) - \frac{k_x}{2} \Delta x \end{aligned} \tag{11}$$

2) Bistatic deformation term: $\psi_2(k_x, \omega; x_0, y_0)$

$$\psi_2(k_x, \omega; x_0, y_0) = -\frac{1}{4} \frac{\left[\left(\frac{\omega+\omega_0}{c/2}\right)^2 - k_x^2\right]^{\frac{3}{2}} \cdot (\hat{x}_1 - \hat{x}_2)^2}{\left(\frac{\omega+\omega_0}{c/2}\right)^2 \cdot (R_{01} \cos\theta_{s1} + R_{02} \cos\theta_{s2})} \tag{12}$$

$$\begin{aligned} & (\hat{x}_1 - \hat{x}_2)^2 \\ & = \Big[R_{01} \sin\theta_{s1} - R_{02} \sin\theta_{s2} \\ & - \frac{k_x}{\sqrt{\left(\frac{\omega+\omega_0}{c/2}\right)^2 - k_x^2}} (R_{01} \cos\theta_{s1} - R_{02} \cos\theta_{s2}) \Big]^2 \end{aligned} \tag{13}$$

4. DOPPLER PROPERTIES

4.1. QUADRATIC APPROXIMATION

For convenience, in the later parts of this paper, the argument list $(x; x_0, y_0)$ is simplified to be (x). So, we use $R_1(x)$ to replace $R_1(x; x_0, y_0)$, *etc.* In low squint and small aperture case, the range equation of bistatic SAR can be supposed to be the sum of two parabolic curves with time (or azimuth).

$$\begin{aligned} R_1(x) \approx & R_{01} - \sin\theta_{s1}(x - x_{01} - \Delta x) \\ & + \frac{1}{2} \frac{\cos^2\theta_{s1}}{R_{01}} (x - x_{01} - \Delta x)^2 \end{aligned} \tag{14}$$

$$R_2(x) \approx R_{02} - \sin\theta_{s2}(x - x_{02}) + \frac{1}{2} \frac{\cos^2\theta_{s2}}{R_{01}} (x - x_{02})^2 \tag{15}$$

Here, for the variable of azimuth is the azimuth length x, rather than the azimuth time, the Doppler properties will be measured using the Doppler wavenumber $k_x(x)$, the Doppler wavenumber centroid $k_{xc}(x)$, and the Doppler wavenumber rate $k_{xr}(x)$. The quadratic approximation model corresponds to a linear FM signal in the time domain.

$$\begin{aligned} k_x(x) = & -\frac{2\pi}{\lambda} \frac{\mathrm{d}R_b(x)}{\mathrm{d}x} = \frac{2\pi}{\lambda} (\sin\theta_{s1} + \sin\theta_{s2}) \\ & - \frac{2\pi}{\lambda} \left[\frac{\cos^2\theta_{s1}}{R_{01}} (x - x_{01} - \Delta x) + \frac{\cos^2\theta_{s2}}{R_{02}} (x - x_{02}) \right] \end{aligned} \tag{16}$$

The Doppler wavenumber centroid is:

$$k_{xc}(x) = \frac{2\pi}{\lambda} (\sin\theta_{s1} + \sin\theta_{s2}) \tag{17}$$

The Doppler wavenumber rate is:

$$k_{xr}(x) = -\frac{2\pi}{\lambda} \left[\frac{\cos^2\theta_{s1}}{R_{01}} + \frac{\cos^2\theta_{s2}}{R_{02}} \right] \tag{18}$$

4.2. NO APPROXIMATION

When the squint angles of the two platforms increase, the quadratic approximation becomes unapplicable. The range history should be expressed in more accurate results, such as four order approximation[5] and the flatten hyperbolic form[4]. By the way, the level of squint in bistatic case should be measured using the squint angles of both platforms.

In this paper we use the flatten hyperbolic model which is an accurate expression of bistatic translational invariant range

Table 1: SIMULATION PARAMETERS

Parameters	Symbol	Quantity
Carrier frequency	f_c	9.6 GHz
Transmitter antenna beamwidth	θ_1	4°
Receiver antenna beamwidth	θ_2	4°
Transmitter height	H_1	20 km
Receiver height	H_2	10 km

history. Using this model, the Doppler signal is similar to sine or polynomial rather than linear. And there is now a stronger cross coupling between range and azimuth. Hence, the Doppler wavenumber is:

$$\begin{aligned} k_x(x) &= -\frac{2\pi}{\lambda}\left[\frac{(x-x_{02})-R_{02}\sin\theta_{s2}}{\sqrt{R_{02}^2+(x-x_{02})^2-2R_{02}(x-x_{02})\sin\theta_{s2}}}\right. \\ &\left.+\frac{(x-x_{01}-\Delta x)-R_{01}\sin\theta_{s1}}{\sqrt{R_{01}^2+(x-x_{01}-\Delta x)^2-2R_{02}(x-x_{01}-\Delta x)\sin\theta_{s1}}}\right] \end{aligned} \tag{19}$$

The Doppler wavenumber centroid expression is the same with the quadratic approximation case (17) and the wavenumber modulation rate is shown in (20).

4.3. RELATIONSHIP BETWEEN DOPPLER PARAMETERS AND SQUINT ANGLES

It is useful to define instantaneous squint angles of the platforms, $\theta_{is1}(x)$ and $\theta_{is2}(x)$, which vary with azimuth. From the geometry configuration and (19), (20), we obtain:

$$k_x(\theta_{is1},\theta_{is2}) = \frac{2\pi}{\lambda}\left(\sin\theta_{is1}+\sin\theta_{is2}\right) \tag{21}$$

$$\begin{aligned} k_{xc}(\theta_{is1},\theta_{is2}) &= \frac{2\pi}{\lambda}(\sin\theta_{is1}|_{\theta_{is1}=\theta_{s1}}+\sin\theta_{is2}|_{\theta_{is2}=\theta_{s2}}) \\ &= \frac{2\pi}{\lambda}(\sin\theta_{s1}+\sin\theta_{s2}) \end{aligned} \tag{22}$$

$$k_{xr}(\theta_{is1},\theta_{is2}) = \frac{2\pi}{\lambda}[\cos\theta_{is1}\theta'_{is1}(x)+\cos\theta_{is2}\theta'_{is2}(x)] \tag{23}$$

Because the instantaneous squint angle and the azimuth coordinate x have a nonlinear relation, (20) and (23) have different meanings to represent the Doppler wavenumber. The simulation parameters are listed in Table 1. Fig.2 shows the relation between k_{xc}, k_{xr} and the squint angles. It can be seen that, receiver squint angle and the one of transmitter play equivalent role in k_{xc}. When $\theta_{s1} = -\theta_{s2}$, k_{xc} is always zero. For the slant ranges are involved in k_{xr}, squint angles of two platforms have different effects to determine k_{xr}. Large slant range means a slow variance versus the instantaneous squint angle.

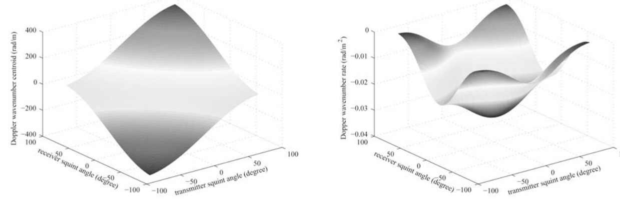

(a) $k_{xc}(\theta_{is1},\theta_{is2})$ (b) $k_{xr}(\theta_{is1},\theta_{is2})$

Fig. 2: Relationship between Doppler wavenumber centroid(a), Doppler wavenumber rate(b) and squint angles.

4.4. THE ACCURACY OF QUADRATIC APPROXIMATION

Next,we will analyze the accuracy of the Doppler parameters with the quadratic approximation.

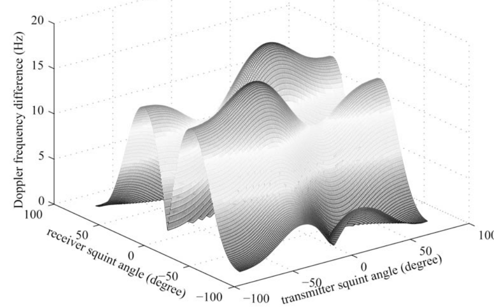

Fig. 3: The difference between the Doppler frequency with no approximation and with quadratic approximation.

In Fig.3, the max error which always occurs at the aperture edge, is sketched with different squint angles, but same azimuth antenna beamwidth, same exposure field. We can find that, when the squint angles exceed certain values, the error does not increases with the squint angles, but deduces. This trend is the same with the monostatic case. Meanwhile, the effect of the squint angles in the difference is also determined by the slant ranges. Large range corresponds less effect. This is because the range dependence of Doppler frequency, which can also be saw when we discuss the azimuth resolution.

5. RESOLUTIONS

5.1. RESOLUTIONS

Supposing the synthetic time is T_s, the Doppler wavenumber bandwidth is:

$$B_d = \int_{-T_s v_a/2}^{T_s v_a/2} k_{xr}(x)dx \tag{24}$$

$$
\begin{aligned}
k_{xr}(x) &= -\frac{2\pi}{\lambda} R_b(x)'' = k_x(x)' \\
&= -\frac{2\pi}{\lambda}\left[\frac{\sqrt{R_{02}^2+(x-x_{02})^2-2R_{02}(x-x_{02})\sin\theta_{s2}}-\frac{(x-x_{02}-R_{02}\sin\theta_{s2})^2}{\sqrt{R_{02}^2+(x-x_{02})^2-2R_{02}(x-x_{02})\sin\theta_{s2}}}}{R_{02}^2+(x-x_{02})^2-2R_{02}(x-x_{02})\sin\theta_{s2}}\right. \\
&\quad \left. + \frac{\sqrt{R_{01}^2+(x-x_{01}-\Delta x)^2-2R_{01}(x-x_{01}-\Delta x)\sin\theta_{s1}}-\frac{(x-x_{01}-\Delta x-R_{01}\sin\theta_{s1})^2}{\sqrt{R_{01}^2+(x-x_{01}-\Delta x)^2-2R_{01}(x-x_{01}-\Delta x)\sin\theta_{s1}}}}{R_{01}^2+(x-x_{01}-\Delta x)^2-2R_{01}(x-x_{01}-\Delta x)\sin\theta_{s1}}\right] \qquad (20)
\end{aligned}
$$

To obtain the Doppler wavenumber bandwidth expression, the sum velocity of two platforms v_a should be used. In the bistatic translational invariant case, the velocities of two platforms are the same. So $v_a = v_1 = v_2$. By the way, v_a should also be used to compute the Doppler frequency parameters from the wavenumber parameters.

The azimuth resolution is [6]:

$$\rho_a = \frac{2\pi}{B_d} \qquad (25)$$

And its direction should be expressed in the direction of the sum velocity.

The range resolution can be obtained easily [6]:

$$\rho_r = \frac{c}{2B\cos\psi/2} \qquad (26)$$

where B is the bandwidth of transmitted signal and ψ is the bistatic angle. The direction of ρ_r is on the sum slant range.

5.2. SQUINT ANGLE AND RESOLUTIONS

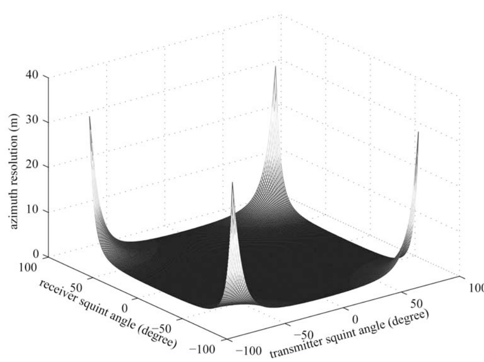

Fig. 4: Relation between azimuth resolution and squint angles.

Bistatic azimuth resolution is determined mostly by three parts: sum velocity, velocity ratio and slant range ratio, which is influenced by the height of platforms and the squint angles[6]. In the bistatic translational invariant case, the velocity ratio is always constant one and the sum velocity is a constant. So, we just consider the relation between the resolution and the squint angles and the heights of platforms. Using the same velocity, same azimuth antenna beamwidth, same beam center location, but different squint angles, different heights, we can get the relation between the azimuth resolution and the squint angles. In Fig.4 the squint angles are less than $80°$. When squint angles both increase to $90°$, the azimuth resolution becomes infinite. We can find, when the squint angles increase, the resolution also get large. Furthermore, squint angles have unequal performances in azimuth resolution, because the instantaneous slant ranges are involved.

6. CONCLUSION

Signal properties of squint mode bistatic SAR translational invariant case have been presented. The accuracy of quadratic approximation is also given. Finally, the relationships between the Doppler properties, azimuth resolution and the squint angles are illustrated. The signal model and the Doppler expressions in this paper are deduced using the complete accurate bistatic range history. So the results are applicable for the large aperture and high squint cases. The analysis in this paper could bring a novel angle of view to study bistatic SAR.

In the future, we will study the imaging algorithms for the large aperture and high squint bistatic SAR both in simulation and using the measured data.

7. REFERENCES

[1] N. J. Willis, *Bistatic radar*, Artech House, Boston, 1991.

[2] G. Krieger, H. Fiedler, and A. Moreira, "Bi- and multistatic sar: potentials and challenges," in *EUSAR 2004*, 2004, pp. 365–370.

[3] J. H. G. Ender, "A step to bistatic sar processing," in *EUSAR 2004*, 2004, pp. 359–364.

[4] O. Loffeld, H. Nies, V. Peters, and S. Knedlik, "Models and useful relations for bistatic sar processing," *Geoscience and Remote Sensing, IEEE Transactions on*, vol. 42, no. 10, pp. 2031–2038, 2004.

[5] K. Eldhuset, "A new fourth-order processing algorithm for spaceborne sar," *Aerospace and Electronic Systems, IEEE Transactions on*, vol. 34, no. 3, pp. 824–835, 1998.

[6] Y. L. Huang, J. J. Wu, J. Y. Yang, and J. T. Xiong, "Analysis of resolutions in bistatic sar," *Chinese Journal of Radio Science*, 2007, in press.